*e*-ISSN 1983-4063 - *www.agro.ufg.br/pat* - Pesq. Agropec. Trop., Goiânia, v. 41, n. 3, p. 336-347, jul./set. 2011

# DOUBLE-RING AND TENSION INFILTROMETER MEASUREMENTS OF HYDRAULIC CONDUCTIVITY AND MOBILE SOIL REGIONS[1]

John M. Köhne[2], José Alves Júnior[3], Sigrid Köhne[4], Bärbel Tiemeyer[5], Bernd Lennartz[6], Jens Kruse[6]


## RESUMO

MEDIDAS DE CONDUTIVIDADE HIDRÁULICA E MOVIMENTO DE ÁGUA NO SOLO POR ANÉIS CONCÊNTRICOS E INFILTRÔMETRO DE TENSÃO

Existem muitas técnicas e métodos de campo para medir e estimar a condutividade hidráulica saturada do solo (*Ks*). Neste estudo, medidas de condutividade hidráulica ($K_s$) e movimento de água no solo, pelos métodos anéis concêntricos (DI) e infiltrômetro de tensão (TI), foram avaliados em solo de textura média (Gleyic Luvisol), em Rostock, na Alemanha. Após obtida a estabilidade de infiltração da água, utilizando-se os métodos DI, TI (sem contato com areia) e $TI_{sand}$ (com contato com areia), três lâminas de 25 mm, 50 mm e 100 mm de solução corada de azul, 2 g $L^{-1}$ Brilliant Blue FCF (BB), foram aplicadas, em diferentes posições, na área. Os resultados mostraram variação nos valores de $K_s$ obtidos por DI de 820-2.020 cm $d^{-1}$, os quais foram de 7 a 13 vezes maiores, quando comparados aos valores com TI, e 12 a 33 vezes maiores, quando comparados com $TI_{sand}$. Para as aplicações de 25 mm e 50 mm de BB, o corante concentrou-se 60% na camada de 25 cm e variou pouco entre os métodos de infiltração. Somente para a lâmina de 100 mm, utilizando-se o método DI, observou-se dispersão do corante, atingindo camadas mais profundas. Assim, observou-se que os valores de $K_s$ e a dispersão de corante dependeram das condições de contorno. Além disto, para o método DI, mais de 90% do corante concentrou-se abaixo da área de infiltração, revelando fluxo vertical preferencial.


PALAVRAS-CHAVE: Fluxo preferencial; transporte de soluto; corante de solo; zona de mobilidade.


## ABSTRACT

There are several field methods and techniques for measuring *Ks*. In this study, double-ring (DI) and tension infiltrometer (TI) infiltration techniques were combined with dye tracer application and compared for estimating $K_s$ and the mobile soil fraction on a structured sandy loam soil (Gleyic Luvisol), in Rostock, Germany. Water was infiltrated into soil by using three methods: DI, TI (without contact with sand), and $TI_{sand}$ (with contact with sand), until steady-state conditions were obtained. At different positions, three pulse depths of 25 mm, 50 mm, and 100 mm, with a 2 g $L^{-1}$ Brilliant Blue (BB) FCF dye solution, were used. The results showed variable $K_s$ values for DI of 820-2,020 cm $d^{-1}$, which were 7 to 13 times higher, when compared to TI values, and 12 to 33 times higher than for $TI_{sand}$. For the 25 mm and 50 mm BB applications, the mobile (dye-stained) soil regions constituted up to 60% in the top 25 cm and varied little, when considered the infiltration methods. Only the 100 mm application, using the DI, yielded significant BB displacement into the subsoil. Hence, both $K_s$ values and their corresponding dye pattern depended on the boundary conditions. For DI, more than 90% of the dye was constrained below the infiltration area, revealing that flow was essentially vertical.


KEY-WORDS: Preferential flow; solute transport; dye tracer; mobile region.

## INTRODUCTION

The saturated hydraulic conductivity ($K_s$) controls, together with the gradient in hydraulic potential, the upper limit of water flow in soils. Thus $K_s$ is an important soil physical property for various agronomic, engineering, and environmental problems. It is also a key parameter in the design and performance assessment of irrigation and drainage systems, earthen waste impoundments,

1. Article submitted on Sept./2010 and accepted for publishing on Aug./2011 (n° PAT 11376/ DOI: 10.5216/pat.v41i3.11376).
2. Helmholtz Centre for Environmental Research (UFZ), Department of Soil Physics, Halle, Germany. *E-mail*: max.koehne@ufz.de.
3. Universidade Federal de Goiás, Escola de Agronomia e Engenharia de Alimentos, Goiânia, GO, Brazil. *E-mail*: jose.junior@pq.cnpq.br.
4. Martin-Luther Universität, Halle, Gemany. *E-mail*: sigrid.koehne@ufz.de.
5. Johann Heinrich von Thünen-Institut, Institut für Agrarrelevante Klimaforschung, Braunschweig, Germany. *E-mail*: baerbel.tiemeyer@auf.uni-rostock.de.
6. University of Rostock, Institute for Land Use, Faculty for Agricultural and Environmental Sciences, Rostock, Germany. *E-mails*: bernd.lennartz@auf.uni-rostock.de, jens.kruse@auf.uni-rostock.de.

waste water leach fields, and many other agricultural, geotechnical, and environmental structures (Reynolds et al. 2000). Furthermore, $K_s$ is an essential parameter in physically-based models for simulating water flow and chemical transport in soils.

There are several field methods and techniques to measure $K_s$. The double-ring infiltrometer (DI) can be used to assess $K_s$ from measuring infiltration at a constant positive pressure equal to the water ponding depth, while the tension infiltrometer (TI) is applied to derive $K_s$ or unsaturated hydraulic conductivity from infiltration measurements performed at zero or negative pressures (White & Sully 1987, Perroux & White 1988, Ankeny et al. 1991). Both DI and TI offer a fast and convenient means for determining $K_s$ and other soil hydraulic properties based on *in situ* infiltration measurements at the soil surface.

Although DI is potentially well suited for measuring the $K_s$ of agricultural soils, it has so far received little field testing or comparison with other methods (Reynolds et al. 2000).

The TI and DI methods can be applied alternately at the same location with minimum disturbance of the infiltration surface, and, for both techniques, the infiltration process is controlled by the pressure head imposed on the soil surface. Consequently, DI and TI techniques should be similar enough to avoid misconceptions arising from method comparison.

The use of tension infiltrometer to measure $K_s$ presents one difficulty, however. Ensuring intimate contact between the soil surface and water source (infiltrometer membrane) is crucial for the estimation of surface soil hydraulic properties from the tension infiltrometer (Perroux & White 1988). The contact sand needed to ensure good hydraulic connection between the infiltrometer and soil can introduce flow impedance effects, at initial high infiltration rates, associated with zero-head and ponded conditions (Reynolds & Zebchuk 1996). The presence of a thin contact sand layer on the soil surface should not practically influence steady-state infiltration rates, provided that the water permeability of the contact material is greater than that of the soil (Vandervaere et al. 2000, Clothier & Scotter 2002). However, in some studies, a decrease in infiltration rates, measured by a tension infiltrometer set at a slightly positive head, was measured in the presence of a contact sand layer (Everts & Kanwar 1993, Schwärzel & Punzel 2007).

Only a few authors have compared DI with TI, for measuring the $K_s$ of agricultural soils (Vanderlinden et al. 1998, Reynolds et al. 2002, Luna-Saez et al. 2005). Generally, the DI method provided larger $K_s$ values than the TI one, except for low-permeability soils, where results were rather similar for DI and TI methods. The explanation suggested is that some macropores, which were conductive under ponded conditions, were inactive when the TI method was applied (Vanderlinden et al. 1998, Reynolds et al. 2002). However, such explanation is difficult to be checked, unless information about preferential macropore flow can be obtained.

Some studies presented derived estimates of macroporosity from water infiltration measurements, at different applied tensions, using the capillary-rise equation (Watson & Luxmoore 1986, Dunn & Philips 1991). Methods based on water flow alone may not provide reliable estimates for preferential flow paths. For example, the $K(h)$ characteristic of sand with continuous pore size distribution and fine-textured soil with macropores may not always be distinguishable. In fine-textured soils, soil structure provides the flow paths associated with the mobile soil water fraction, which is crucial for estimating effective pore water and solute transport velocities. Mobile soil water contents were estimated in a combined tension infiltration and bromide tracer method (Clothier et al. 1992, Reynolds 2006). However, the spatial resolution for the latter method depends on the density of the sampling grid, and resulting mobile water contents are valid only within simplifying assumptions.

Maybe the most direct way to determine preferential flow path distribution, and infer mobile soil regions *in situ*, is the use of dye tracers. Images of dye patterns can identify the transport behaviour in much greater detail than it is possible with a conservative tracer, using current sampling methodologies (Kasteel et al. 2002, Öhtröm et al. 2004). For non-linear weakly adsorbed dyes (solute transport behaviour affected by the input concentration), with a maximum adsorption capacity in a particular soil, continuous application, at high concentrations, will lead to nearly conservative movement of the non-sorbed dissolved dye fractions (Perillo et al. 1998, Kasteel et al. 2002). Just a few studies (Lin & McInnes 1995) have evaluated the potential of dye infiltration measurements at constant-head conditions to derive both hydraulic parameters and information about flow paths.

In this study, constant-head (ponded or zero tension) infiltration of water and dye tracer application were combined in order to simultaneously estimate $K_s$ and the flow path distribution according to depth, which gives an estimate for the mobile soil region (water movement).

The objectives of this study were to measure $K_s$, using DI (ponded) and TI (zero-head), without or with contact sand ($TI_{sand}$), and to verify whether potential differences among resulting $K_s$ values can be explained by flow pattern, as obtained from dye tracing; quantify vertical and horizontal flow components, by using TI, $TI_{sand}$ and DI; and assess the effect of infiltrating different dye solution pulse depths (25 mm, 50 mm, and 100 mm) at the surface and subsoil on the dye pattern.

## MATERIAL AND METHODS

The experiment was carried out in Dummerstorf, located around 15 km southeast of Rostock (North-Eastern Germany), on arable land, in a Pleistocene lowland landscape, in 2005. Long-term mean annual precipitation, potential evapotranspiration (modified Penman) and temperature are 665 mm, 561 mm, and 8.2°C, respectively. The crop rotation at the experimental field included corn (*Zea mays*, harvest 2003), winter wheat (*Triticum aestivum*, harvest 2004), and winter rape (*Brassica napus*, harvest 2005). The agricultural field was artificially drained with tile and ditch drainage and subjected to conventional tillage. The sandy loam soil was classified as Gleyic Luvisol, according to WRB (Map of World Soil Resources) classifications (FAO 1998), and average soil physics properties in conformity to Tiemeyer et al. (2005).

One location was selected within the Dummerstorf field for measuring the infiltration of water and Brilliant Blue FCF dye solution (BB). The plot was located at a hilltop position. The soil had been ploughed and the topsoil compacted using rollers, a few weeks prior to the infiltration tests. However, there was no evidence of a plough compaction pan.

Four plots, covering a 5 m x 6 m area each, were used. A total of nine locations in each plot, i.e., combinations of DI, TI, and $TI_{sand}$ methods, for 25 mm, 50 mm, and 100 mm BB infiltration, were selected on a regular grid, on the soil surface, and one additional set (25 mm; DI, TI, and $TI_{sand}$) was selected on the subsoil, at 40 cm depth. Additionally, two replicate DI infiltration measurements were performed on the surface and subsoil with water only. To prepare the soil for the infiltration measurement, newly grown winter rape plants (0.15 m high) were carefully trimmed to the soil surface.

For DI infiltration, the inner and outer steel rings of 0.2 m and 0.4 m diameter, respectively, were driven concentrically about 0.05 m deep into the soil, with minimum soil disturbance. Adjacent to the DI positions, infiltration experiments were carried out using a custom-made TI, with a 0.2 m diameter disk. A single ring was used for TI and $TI_{sand}$ measurements, to prevent surface runoff. The TI tests were performed with the infiltrometer membrane in direct contact with the carefully leveled soil, while $TI_{sand}$ infiltrations were carried out by using a thin layer (5 mm) of fine sand (0.1 mm particle sizes) added to the soil surface, to ensure a level base and best contact between infiltrometer disk and the field soil.

First, tap water was infiltrated, during 45 minutes, for all tests. That provided comparable initial conditions (initial water content and established flow paths) for subsequent BB transport, at the different locations. Steady-state flow conditions were reached within 5-20 minutes, for all infiltrations. The final steady-state infiltration rate was calculated as an average of the last five to ten measurements taken at 1 minute intervals. A rather small water depth of about 0.03 m was applied to the inner and outer rings of the DI, to minimize the differences between ponded boundary conditions, for DI, and zero applied pressure for TI and $TI_{sand}$.

After establishing steady-state water flow, a particular infiltrometer was quickly replaced by another one pre-filled with Brilliant Blue solution, at the concentration $C_o = 2.0$ g $L^{-1}$. Three different pulse levels of 25 mm, 50 mm, and 100 mm of this BB solution, respectively, were infiltrated. The 25 mm pulse was expected to characterize only the top soil horizon, while the larger pulses were expected to stain both upper and lower soil horizons. Initial and final water contents were estimated by using a time domain reflectometry (TDR) probe (probes of 0.2 m long).

On the day following a particular infiltration and dye application, vertical soil profiles of 0.6 m x 0.6 m, 0.8 m x 0.8 m, and 1.0 m x 1.0 m were photographed for the 25 mm, 50 mm, and 100 mm of dye applications, respectively. To assess the extent of horizontal dye movement, 7 vertical

profiles were prepared outside and within each dye infiltration area, ranging between ±0.3 m and ±0.2 m horizontal distances from the centre (boundaries) of the BB infiltration area, at 0.1 m intervals: 0.3 m, 0.2 m, 0.1 m, 0.0 m (centre), -0.1 m, -0.2 m, -0.3 m. The soil profiles were photographed in a single white tent fabric layer for diffusing light conditions. The photographs were taken with a Canon EOS Digital Colour Camera, with 8 mega-pixels resolution. The camera was mounted on a tripod at a fixed height equal to the centre of each soil profile and a fixed distance to the soil profile of 1.0 m.

For DI, the steady-state vertical water flux through homogeneous soil below the inner ring, kept at the same small water ponding depth as the outer ring, was driven by gravity only at a unit hydraulic gradient. The steady-state vertical water flux under these conditions corresponds to the infiltrability, defined as the flux (or rate) of water infiltration into soil, when water, at atmospheric pressure, is maintained on the atmosphere-soil boundary, with the flow direction being one-dimensionally downward (SSSA 2005). It follows the Darcy's law, which states that the infiltrability should be approximately equal to the field-saturated $K_s$ value, i.e., the maximum $K_s$ value to be expected for infiltration. Due to air inclusions, the field-saturated $K_s$ value may be below the theoretical maximum value for a completely saturated soil. Since air inclusions affect DI and TI methods in a similar way, it is implicitly understood, throughout this paper, that $K_s$ refers to the field-saturated property.

For TI, the infiltrability is additionally affected by lateral capillary forces, since the water flow underneath the circular infiltration area is not vertically confined. In order to obtain comparable values for $K_s$, from the different infiltration methods, one has to account for the three-dimensional flow underneath the TI disk (Wooding 1968, Ankeny et al. 1991). The sorptivity, $S$ ($LT^{-2}$), characterizes the effect of capillary forces on water infiltration. Values for $S$ were estimated at the beginning infiltration stages, when the capillary forces were still dominating over gravity, and where gravity and lateral flow effects can often be neglected (White & Sully 1987). In this early phase, the cumulative infiltration depth, $I$ (L), is approximately proportional to the sorptivity x square root of time (Philip 1969, Mollerup 2007).

For TI and the steady-state infiltration into a homogeneous soil, the steady infiltration rate ($q_\infty$, cm $d^{-1}$) and hydraulic conductivity ($Ks$, cm $d^{-1}$), from a disc at zero tension, were calculated by using the Wooding's (1968) equation:

$$q_\infty = K_s + \frac{4\varphi_s}{\pi}\frac{1}{r}$$

where $\varphi_s$ is the matrix flux potential ($L^2T^{-1}$) (Gardner 1958) and $r$ the infiltrometer disk radius (L).

Photos were taken on the morning following infiltration, i.e., about 15 hours after stopping infiltration. Since the camera was always positioned in the centre of the area of interest, with a distance to the imaged surface of 1.0 m, geometric distortions were minimal. For each profile, an image of the Brilliant Blue FCF dye pattern was analysed. After conversion to black-and-white bitmap images, the depth distribution of dye coverage beneath and outside the cross sections of the infiltration areas (0.2 m) was calculated.

As a first-order approximation, the mobile soil fraction can be set equal to the dye coverage, unless there is substantial lateral diffusion. Visual evaluation at the trench face revealed that lateral diffusion from preferential flow paths in the subsoil, within 15 hours, was minimal in this soil (just a few mm). In the ploughed top soil, where solute transport is more uniform, lateral diffusion is of limited importance as well. Hence, for this soil, lateral dye diffusion could be neglected, for the purpose of estimating a conservative (upper limit) estimate for the mobile soil fraction. An estimate for the mobile soil water content, in a two-region model (van Genuchten & Wierenga 1976 apud Oberdorster et al. 2010), is obtained by the mobile soil fraction x its porosity.

## RESULTS AND DISCUSSION

The values for the steady state flow rate ($q_\infty$), sorptivity ($S$), and hydraulic conductivity ($K_s$) are present in Table 1. In the top soil horizon, values for $q_\infty$, $K_s$, and $S$ were quite variable, but always higher for DI. For instance, the $q_\infty$ values were decreasing in the sequence DI (819-1,810 cm $d^{-1}$), TI (134-241 cm $d^{-1}$), and $TI_{sand}$ (71-171 cm $d^{-1}$). The smaller $q_\infty$ values for $TI_{sand}$, as compared to TI, were not caused by the contact sand $K_s$ value (≈ 550 cm $d^{-1}$). Pressure losses across the thin sand layer may be a possible explanation.

The very large $S$ values for DI are only listed for completeness and are certainly not realistic, since ponded flow conditions caused even the initial infiltration to be strongly affected by gravity, which

Table 1. Average of results for steady state flow ($q_\infty$), sorptivity ($S$), and hydraulic conductivity ($K_s$), for infiltration tests using double-ring infiltrometer (DI), tension infiltrometer with contact sand ($TI_{sand}$), and tension infiltrometer with disk directly placed on the soil (TI) (Rostock, Germany, 2005).

| Location (Pulse depth) | Infiltration method | Steady-state flow rate | Sorptivity¶ | Hydraulic conductivity ¶ | Percentage of lateral flow |
|---|---|---|---|---|---|
| | | ($q_\infty$) | (S) | $K_s$ | $100(\theta_\infty - K\sigma)/\theta_\infty$ |
| | | cm $d^{-1}$ | cm $d^{-1/2}$ | cm $d^{-1}$ | % |
| | | *Surface* | | | |
| 25 mm | DI | 819 | 73.2 | 819 | 0 |
| | TI | 134 | 7.5 | 113 | 16 |
| | $TI_{sand}$ | 71 | 5.2 | 59 | 17 |
| 50 mm | DI | 2015 | 253.1 | 2015 | 0 |
| | TI | 167 | 7.3 | 147 | 12 |
| | $TI_{sand}$ | 92 | 9.0 | 61 | 34 |
| 100 mm | DI | 1810 | 231.8 | 1810 | 0 |
| | TI | 241 | 12.3 | 184 | 24 |
| | $TI_{sand}$ | 171 | 8.8 | 142 | 17 |
| | | *Subsoil*§ | | | |
| 25 mm | DI | 421 | 34.2 | 421 | 0 |
| | TI | 125 | 6.3 | 110 | 12 |
| | $TI_{sand}$ | 26 | 1.9 | 24 | 8 |

§ 0.4 m depth below surface. ¶ Since gravity flow was not considered in the estimation of sorptivity, $S$ values represent upper constraints, while, for TI and $TI_{sand}$, $K_s$ represents lower constraints of the true values.

was neglected in the calculation of $S$. Moreover, while the estimated values for $S$, for $TI_{sand}$, might be expected to be affected by contact sand properties, $S$ values did not differ significantly between TI and $TI_{sand}$. Therefore, the estimated $K_s$ values were decreasing in the same sequence of DI, TI, and $TI_{sand}$, as well as the $q_\infty$ values (Table 1). The estimated reduction between $q_\infty$ and $K_s$, due to lateral flow, as caused by water sorption, ranged 12-34%.

For the subsoil, values for $q_\infty$ and $K_s$ were somewhat smaller ($\leq$ 421 cm $d^{-1}$), but the same decreasing values sequence was noticed for DI, TI, and $TI_{sand}$. The estimated lateral water sorption losses amounted to around 10% (Table 1).

The dye pattern and the vertical distribution of the dye coverage beneath the infiltration area are illustrated in Figures 1 to 3, for the different tests. The lower horizontal axes represent profile width, the upper horizontal axes show dye coverage beneath the infiltration area, and the vertical axes show the depth. The top, middle, and bottom rows of each figure show the profiles at -10 cm, 0 cm, and 10 cm horizontal distance from an infiltration centre. No results are shown for the -0.3 m, -0.2 m, 0.2 m, and 0.3 m profiles, since only a few small dye spots were observed at those distances from the infiltration area. Hence, lateral transport distances were essentially lower than 0.2 m, for all tests.

For the 25 mm application, Brilliant Blue was mostly confined to the upper soil layer, with 100%, 98.5%, and 99.9% of dye for DI, TI, and $TI_{sand}$, respectively, residing within the 0.0-0.4 m depth (Table 2, Figure 1).

For the soil profile intersecting the infiltration area at its centre (0.0 m), BB was horizontally concentrated underneath the application (0.2 m diameter), with 95.0%, 71.5%, and 74.9% of the total dye coverage for DI, TI, and $TI_{sand}$, respectively. The profiles taken at the infiltration area margins (+0.1 m and -0.1 m distances from the centre) also revealed the larger horizontal flow component beneath the TI and $TI_{sand}$ (Figure 1).

This shows that infiltration beneath the inner ring of the DI was mostly confined to the vertical direction, as expected, while, for TI and $TI_{sand}$, considerable amounts (25-28%) of the dye moved horizontally. In the top 20 cm, high dye coverage of about 60%, in the central soil profiles, revealed that most of the soil water was mobile in the topsoil. Moreover, a slight trend of increasing main dye mass depth, while increasing $K_s$ values, was observed: the depth below which dye coverage underneath the infiltration area (central cross-section at 0.0 m) drops below 5% was 0.18 m, for TI and $TI_{sand}$, but 0.27 m for DI, which had the largest $K_s$ value (Table 1, Figure 1).

Table 2. Distribution of horizontal and vertical dye coverage average (%) in top and subsoil profiles, as obtained for the different infiltration methods (DI, TI, and $TI_{sand}$), by using different pulse depths of applied Brilliant Blue solution (25 mm, 50 mm, and 100 mm) (Rostock, Germany, 2005).

| Location Pulse depth | Infiltration method | Dye coverage | | | |
|---|---|---|---|---|---|
| | | Topsoil (0-0.4 m) | Pulse depth | Infiltration method | Topsoil (0-0.4 m) |
| | | Percentage of the total observed dye-stained area | | | |
| | | *Surface* | | | |
| 25 mm | DI | 100.0 | 0.0 | 95.0 | 5.0 |
| | TI | 98.5 | 1.5 | 71.5 | 28.5 |
| | $TI_{sand}$ | 99.8 | 0.2 | 74.9 | 25.1 |
| 50 mm | DI | 99.8 | 0.2 | 97.0 | 3.0 |
| | TI | 100.0 | 0.0 | 92.6 | 7.4 |
| | $TI_{sand}$ | 100.0 | 0.0 | 83.9 | 16.1 |
| 100 mm | DI | 81.3 | 18.7 | 91.1 | 8.9 |
| | TI | 98.0 | 2.0 | 98.2 | 1.8 |
| | $TI_{sand}$ | 98.8 | 1.2 | 98.9 | 1.1 |
| | | *Subsoil* | | | |
| Location Pulse depth | Infiltration method | subsoil (0.4-0.7 m) | Pulse depth | Infiltration method | subsoil (0.4-0.7 m) |
| | | Percentage of the total observed dye-stained area | | | |
| 25 mm | DI | 48.5 | 51.5 | 87.2 | 12.8 |
| | TI | 34.5 | 65.5 | 90.8 | 9.2 |
| | $TI_{sand}$ | 76.1 | 23.9 | 66.0 | 34.0 |

For the 50 mm application, BB was still vertically concentrated on the top soil layer, with 99.9%, 99.6%, and 99.9% of dye coverage. Horizontally, BB was concentrated under the application area, with 97.0%, 92.6%, and 83.9% of dye coverage for DI, TI, and $TI_{sand}$, respectively (Table 2, Figure 2). The maximum horizontal movement of Brilliant Blue, as judged from small dye spots representing preferential flow paths, was up to 0.2 m from the margins of the application area. Surprisingly, the 50 mm application did not obviously cause higher dye coverage or deeper dye movement than the 25 mm one. Furthermore, as opposed to the observations made for the 25 mm application, no relation between depth of dye movement and $K_s$ was identified. For DI, the small dye coverage in the top soil horizon suggests that most of the dye was lost via preferential flow paths. Many of such dye-stained paths only appeared as tiny spots at their intersections with the vertical soil profile.

For the 100 mm application, BB was, once again, vertically concentrated on the top soil horizon (0.0-0.4 m), with 81.2%, 98.0%, and 98.8% of dye coverage for DI, TI, and $TI_{sand}$, respectively (Table 2, Figure 3). However, the fraction of BB that moved to larger depths significantly increased for DI, as compared to the 25 mm and 50 mm applications, and was also higher than for TI and $TI_{sand}$.

Furthermore, the DI test revealed a clear separation between the matrix-dominated transport zone in the top soil horizon, with large dye coverages of 40-80%, suggesting larger mobile water fractions, and the preferential flow zone in the subsoil, with small dye coverages between 1% and 20%, representing earthworm burrows, root channels, and interaggregate zones.

The TI and $TI_{sand}$ techniques (and DI, for 25 mm and 50 mm BB) did not show the preferential flow pattern in the subsoil. This suggests that only (prolonged) ponding at the soil surface could initiate significant macropore flow in the subsoil. The increase of the percentage in dye coverage in larger depths was also reflected by the larger $K_s$ value for DI (Table 2, Figure 3).

In general, in this study, very little horizontal dye movement was observed for TI methods, and the dye was mostly concentrated under the infiltration area with 91.1%, 98.2%, and 98.9% of dye coverage, using DI, TI, and $TI_{sand}$, respectively (Table 2). A plausible explanation for the predominantly vertical dye displacement, even for TI and $TI_{sand}$ techniques, would be a larger anisotropy of $K_s$, due to more continuous vertical flow paths, at this part of the plot. The $K_s$ values for TI and $TI_{sand}$ were the largest ones observed for surface infiltrations (Table 1). The negligible lateral dye losses suggest that estimates

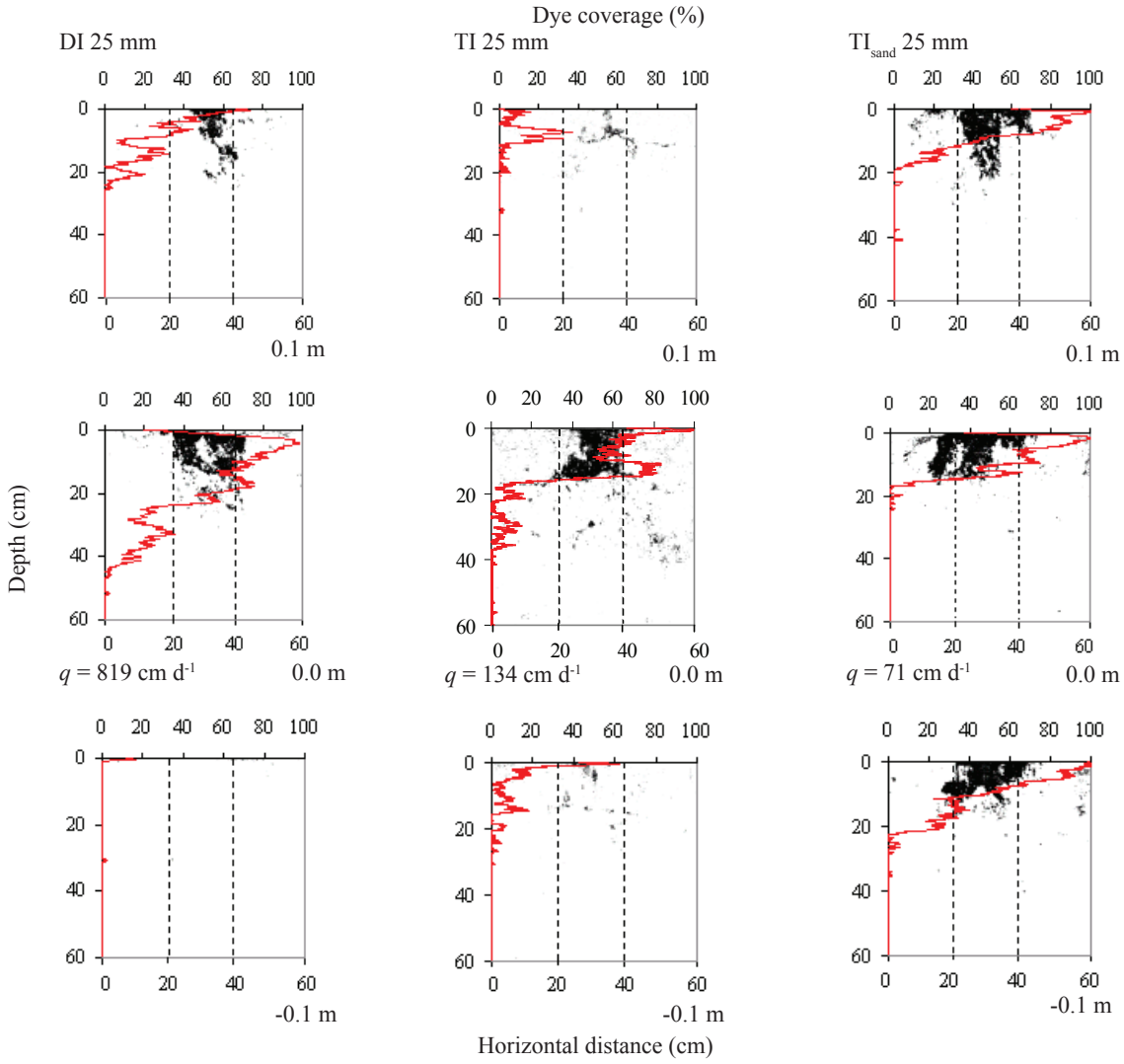


Figure 1. Average of dye patterns resulting from 25 mm Brilliant Blue infiltration, using the double-ring infiltrometer (DI - left column), tension infiltrometer without contact sand (TI - middle column) and with contact sand (TI$_{sand}$ - right column). The soil profiles of 0.6 m x 0.6 m were at distances of 0.1 m (top row), 0.0 m (middle row), and -0.1 m (bottom row), from the infiltration areas (Rostock, Germany, 2005).

for sorptivity and lateral water losses of around 20% (Table 1) were unrealistically high.

Infiltration on the subsoil horizon of 25 mm BB showed a dye pattern characterized by preferential flow paths, predominantly earthworm burrows, for all infiltration methods (Figure 4). This reveals that zero-head infiltration (TI and TI$_{sand}$) was sufficient to create substantial macropore flow only when infiltrating directly in the subsoil. Hence, for TI and TI$_{sand}$, the dye pattern in the subsoil was a function of the location of the infiltration source, whereas, for DI, it seemed fairly independent (Figures 3 and 4).

For DI, a more or less even depth distribution was found with about half of the BB in the 0.4-0.7 m depth and half in the 0.7-1.0 m depth (Figure 4, Table 2). The TI and TI$_{sand}$ techniques showed varied distributions of dye coverage in depth. For TI, 34.5% of BB was in the 0.4-0.7 m depth and 65.5% was in the 0.7-1.0 m depth, while, for TI$_{sand}$, 76.1% was in the 0.4-0.7 m depth and 23.9% in the 0.7-1.0 m depth. However, this difference between TI and TI$_{sand}$ approaches may be mostly due to the heterogeneity of the macropore distribution in the subsurface layer.

When comparing TI with TI$_{sand}$ measurements, mostly larger $K_s$ values were found for TI (Table 1), in agreement with slightly larger fractions of BB displaced to larger depths (Table 2).

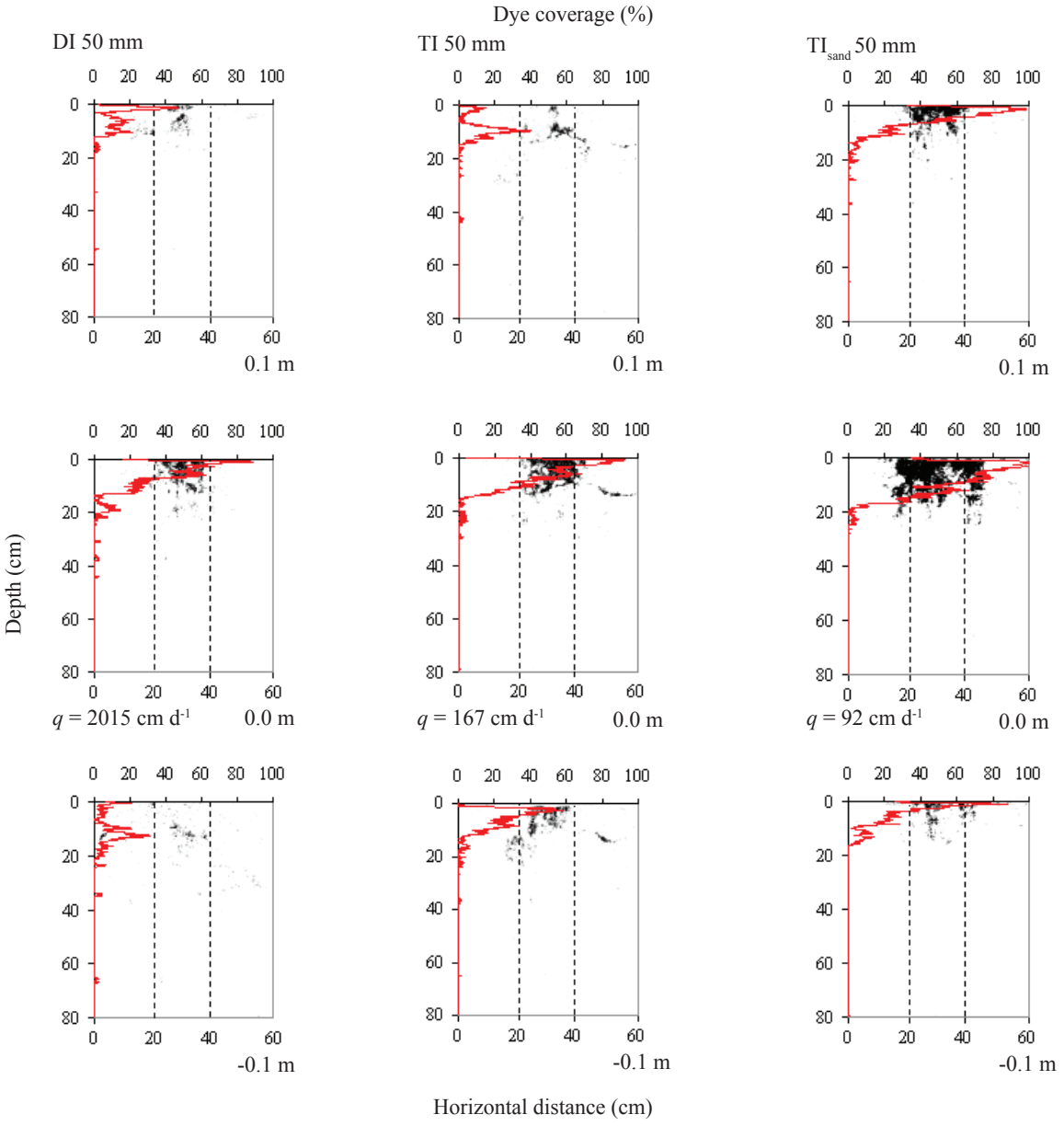


Figure 2. Dye patterns average resulting from 50 mm Brilliant Blue infiltration, using the double-ring infiltrometer (DI - left column), tension infiltrometer without contact sand (TI - middle column) and with contact sand ($TI_{sand}$ - right column). The soil profiles of 0.6 m x 0.8 m were at distances of 0.1 m (top row), 0.0 m (middle row), and -0.1 m (bottom row) from the infiltration areas (Rostock, Germany, 2005).

Additionally, we attempted to continuously monitor water and BB infiltration at the trench face, by using depth-staggered TDR probes. However, in all tests, inevitably BB leached from macropore intersections with the trench face. Therefore, real-time transport monitoring was not possible.

The $K_s$ values measured for infiltration at the surface decreased in the sequence DI, TI, and $TI_{sand}$. The larger values for DI, rather for TI techniques, are in accordance with previous findings (Vanderlinden et al. 1998, Reynolds et al. 2002, Luna-Saez et al. 2005). However, for the 25 mm and 50 mm applications, the rather similar dye patterns could not explain differences between the higher $K_s$ obtained for ponded (DI), as compared to the zero-head (TI and $TI_{sand}$) infiltration methods. The 25 mm and 50 mm applications were characterized by more than 98% of the BB dye residing in the upper soil horizon.

The 100 mm application using the DI yielded significant (almost 20%) BB displacement into the

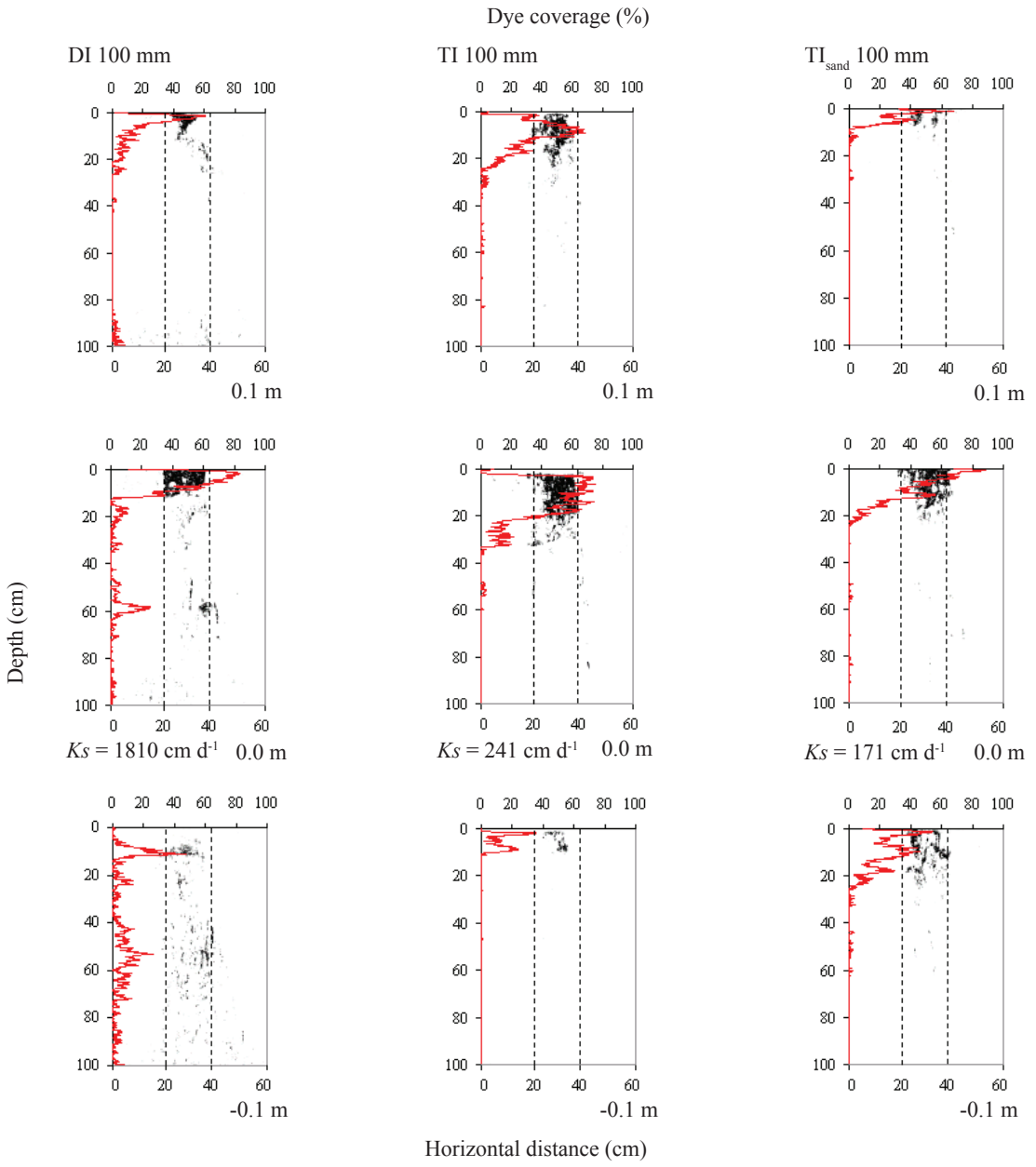


Figure 3. Dye patterns average resulting from 100 mm Brilliant Blue infiltration, using the double-ring infiltrometer (DI - left column), tension infiltrometer without contact sand (TI - middle column) and with contact sand ($TI_{sand}$ - right column). The soil profiles of 0.6 m x 1.0 m were at distances of 0.1 m (top row), 0.0 m (middle row), and -0.1 m (bottom row) from the infiltration areas (Rostock, Germany, 2005).

subsoil layer below 40 cm depth, whereas TI and $TI_{sand}$ resulted in only 1-2% BB displacement into the subsoil. It can be concluded that prolonged ponding at the soil surface was required to initiate significant macropore flow in the subsoil. For this test, the larger dye coverage in the subsoil was reflected by larger $K_s$ values for DI than for TI and $TI_{sand}$.

For infiltration of 25 mm BB directly in the subsoil, ponded and zero-head techniques resulted in similar preferential dye patterns with coverage (mobile fractions) mostly below 10%, in accordance with the subsoil dye pattern obtained with the DI 100 mm surface application. However, the relatively similar dye patterns appear to be in contradiction with dissimilar $K_s$ values for DI, TI, and $TI_{sand}$. More detailed tests involving horizontal dye profiles may be necessary to identify potential relations between dye patterns and $K_s$, for different infiltration techniques.

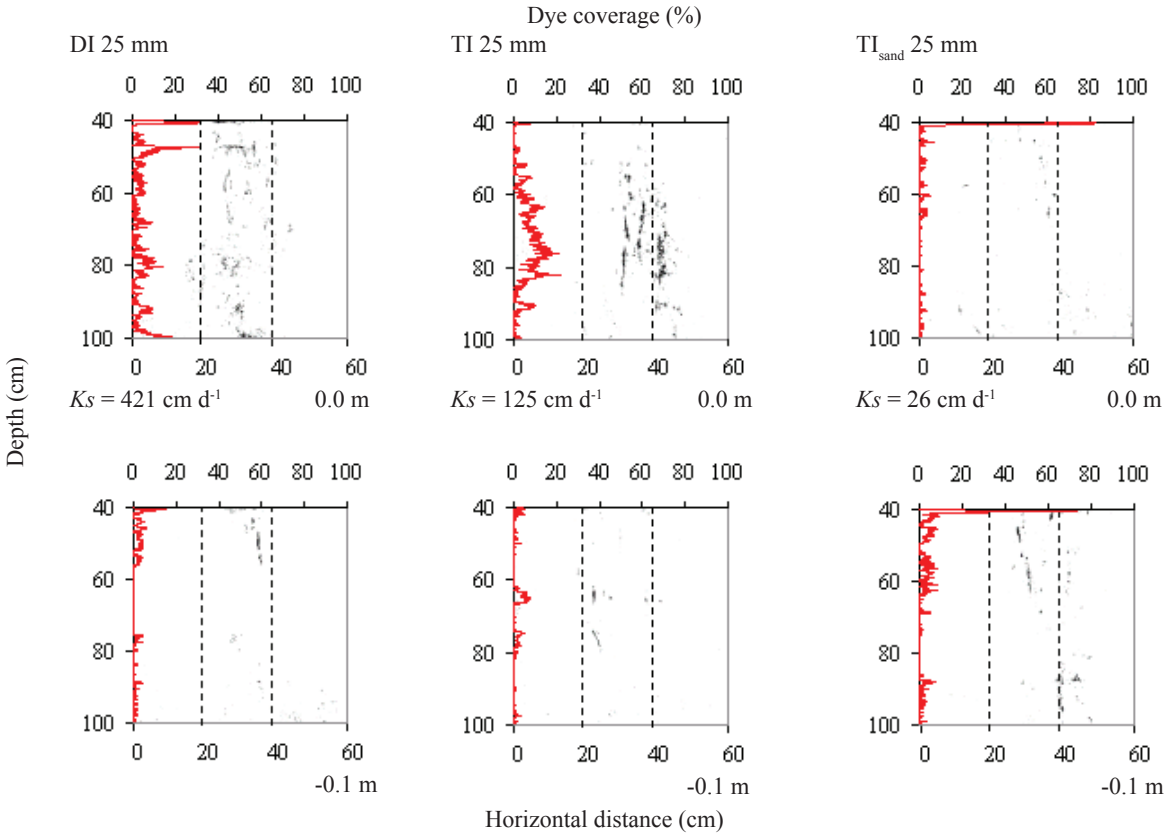


Figure 4. Dye patterns average in subsoil (0.4-1.0 m) profiles of 0.6 m x 0.6 m, at distances of 0.0 m (middle row), and -0.1 m (bottom row) from the infiltration areas, after infiltration of 25 mm of Brilliant Blue, using the double-ring infiltrometer (DI - left column), tension infiltrometer without contact sand (TI - middle column) and with contact sand ($TI_{sand}$ - right column) (Rostock, Germany, 2005).

Furthermore, although the $K_s$ value (or steady-state water flux) for DI was considerably smaller for infiltration into the subsoil than at the surface, this drop in $K_s$ between top/subsoil horizons was not reflected in a decrease over time of the infiltration rate measured at the soil surface. Some lateral divergence of flux must have taken place at the layer interface, to compensate the decrease in $K_s$.

This interpretation is supported by a tendency for larger dye spreading in the subsoil, for the 50 cm depth (i.e., directly below the boundary sub/topsoil, at 40 cm depth), for the DI 100 mm test (Figure 2). Consequently and unfortunately, it would be difficult to obtain $K_s$ values for both layers by infiltration measurements at the surface only, even if $K_s$ values are significantly different for the layers. Only if lateral divergence of flux is restricted, there will be a noticeable infiltration drop at the surface, as measured by Lin & McInnes (1995), for infiltration into a heavy clay soil with slickenside features.

All surface infiltration techniques gave dye-stained (mobile) soil fractions of about 60% in the upper 25 cm of the topsoil horizon. Below this depth, the dye pattern changed from predominantly dye-stained (topsoil) to highly localized spots and lines covering 10% (or less) of the subsoil (DI), characterizing preferential flow paths. Hence, pore water velocity may be almost twice as fast in the topsoil (and even faster in the subsoil) than it would be estimated by using the $K_s$ value and assuming flow through the total soil cross-section.

Vertical and horizontal flow components beneath the TI, $TI_{sand}$, and DI were investigated. As expected, for DI, flow was essentially vertical, with more than 95% of dye coverage being concentrated beneath the infiltration area, for the 25 mm and 50 mm applications, where flow was mainly in the top soil horizon. Dye coverage was still 91% for the 100 mm application, where some lateral losses may have occurred at the transition from topsoil to

the subsoil, with smaller $K_s$. Lateral losses for TI and $TI_{sand}$ were highly variable between infiltration locations and ranged between only 1% (100 mm test) and almost 30% (25 mm test). Since TI techniques do not force infiltration into the vertical direction, lateral spreading was presumably only restrained by the existence of continuous vertical flow paths.

Several previous studies support our findings. Vanderlinden et al. (1998) compared TI and DI infiltration measurements beneath and outside the olive-canopy, in order to detect differences in $K_s$. The DI method gave $K_s$ values whose geometric means (459 cm $d^{-1}$ under and 64.8 cm $d^{-1}$ outside the canopy) were one order of magnitude larger than corresponding values (9.5 cm $d^{-1}$ and 6.9 cm $d^{-1}$, respectively), for the TI method. The larger values for the infiltration positions under canopy were attributed to the higher macroporosity of the more protected soil. Moreover, the differences among $K_s$ values derived with DI and TI were also more pronounced for the (macroporous) soil under canopy (Vanderlinden et al. 1998). The latter result was confirmed by Reynolds et al. (2002), who found lower values of $K_s$ for the TI than for a single-ring pressure (ponded) infiltrometer, for high-permeability soils without tillage, while, for low-permeability soils, results were rather similar. As a possible reason, restricted operation of surface-vented macropores, cracks, or other preferential flow zones under the TI infiltration surface were hypothesized, particularly when using contact material (Reynolds et al. 2002). Higher $K_s$ values for DI, as compared to TI, were also obtained by Luna-Saez et al. (2005).

Considerable lateral dye movement in cracked clay soil beneath the disc of a TI, even at negative supply potentials of -0.03 m, was also found by Lin & McInnes (1995). The dye was found in much larger depths than it would be expected, assuming uniform flow and the measured $K_s$ and water content values (Lin & McInnes 1995). These results very obviously show that traditional tension or pressure infiltration data, in case of structured soils, can be used for predicting water flow velocity or advective transport, unless information about the mobile soil region is added.

## CONCLUSIONS

1. The $K_s$ value, or infiltrability, was found to be one order of magnitude larger for ponded, as compared to zero-head conditions.
2. The use of contact sand beneath the infiltration disk decreased the $K_s$ value by one factor out of two (measurement on soil surface) or five (infiltration on subsoil).
3. The mobile pore network, as inferred from the dye pattern, showed to be, for the topsoil horizon, essentially independent of the infiltration method, but, for the subsoil, it strongly depended on the cumulative infiltration and imposed pressure head.
4. The dye-stained fractions photographed 15 hours after the infiltration test revealed only little lateral diffusion in the subsoil, where they could be used as a conservative (upper limit) estimate of the mobile soil region.
5. The DI estimation of the $K_s$ value strongly relies on the assumption of vertical flow. For the structured sandy loam field soil (Gleyic Luvisol), dye tracer results confirm that flow beneath DI is predominantly (> 90%) vertical. For the TI and $TI_{sand}$ approaches, lateral dye losses in this study were highly variable and constituted up to 30% of the total dye coverage.

## REFERENCES

ANKENY, M. D. et al. Simple field method for determining unsaturated hydraulic conductivity. *Soil Science Society of America Journal*, Madison, v. 55, n. 2, p. 467-470, 1991.

CLOTHIER, B.; SCOTTER, D. Unsaturated water transmission parameters obtained from infiltration. In: TOPP, G. C.; DANE, J. H. (Eds.). *Methods of soil analysis*. Madison: Soil Science Society of America, 2002. p. 879-888.

CLOTHIER, B. E.; KIRKHAM, M. B.; McLEAN, J. E. *In situ* measurement of the effective transport volume for solute moving through soil. *Soil Science Society of America Journal*, Madison, v. 56, n. 1, p. 733-736, 1992.

DUNN, G. H.; PHILLIPS, R. E. Macroporosity of a well-drained soil under no-till and conventional tillage. *Soil Science Society of America Journal*, Madison, v. 55, n. 2, p. 817-823, 1991.

EVERTS, C. J.; KANWAR, R. S. Interpreting tension-infiltrometer data for quantifying soil macropores: some practical considerations. *Transactions of the ASAE*, St. Joseph, v. 36, n. 2, p. 423-428, 1993.

FOOD AND AGRICULTURE ORGANIZATION (FAO). *World reference base for soil resources*. Rome: FAO, 1998.

GARDNER, W. R. Some steady state solutions of unsaturated moisture flow equations with applications to

evaporation from a water table. *Soil Science*, Philadelphia, v. 85, n. 1, p. 228-232, 1958.

KASTEEL, R.; VOGEL, H. J.; ROTH, K. Effect of non-linear adsorption on the transport behaviour of Brilliant Blue in a field soil. *European Journal of Soil Science*, Oxford, v. 53, n. 1, p. 231-240, 2002.

LIN, H. S.; McINNES, K. J. Water flow in clay soil beneath a tension infiltrometer. *Soil Science*, Philadelphia, v. 159, n. 6, p. 375-382, 1995.

LUNA-SAEZ, D.; SÁNCHEZ-REYES, C.; MUÑOZ-PARDO, J. Methods for measuring field-saturated hydraulic conductivity. *Tecnología y Ciencias del Agua*, Jiutepec, v. 20, n. 2, p. 95-107, 2005.

MOLLERUP, M. Philip's infiltration equation for variable-head ponded infiltration. *Journal of Hydrology*, Amsterdam, v. 347, n. 1-2, p. 173-176, 2007.

OBERDORSTER, C. et al. Investigating preferential flow processes in a forest soil using time domain reflectometry and electrical resistivity tomography. *Vadose Zone Journal*, Madison, v. 9, n. 2, p. 350-361. 2010.

ÖHTRÖM, P. et al. Characterizing unsaturated solute transport by simultaneous use of dye and bromide. *Journal of Hydrology*, Amsterdam, v. 289, n. 1, p. 23-35, 2004.

PERILLO, C. A. et al. Flow velocity effects on the retardation of FD&C blue n. 1 food dye in soil. *Soil Science Society of America Journal*, Madison, v. 62, n. 1, p. 39-45, 1998.

PHILIP, J. R. Theory of infiltration. *Advances in Hydroscience*, Varsóvia, v. 5, n. 1, p. 215-296, 1969.

PERROUX, K. M.; WHITE, I. Design for disc permeameters. *Soil Science Society of America Journal*, Madison, v. 52, n. 1, p. 1205-1215, 1988.

REYNOLDS, W. D. Tension infiltrometer measurements: implications of pressure head offset due to contact sand. *Vadose Zone Journal*, Madison, v. 5, n. 4, p. 1287-1292, 2006.

REYNOLDS, W. D.; ELRICK, D. E.; YOUNGS, E. G. Single-ring and double-or-concentric-ring infiltrometer. In: DANE, J. H.; TOPP, G. C. (Eds.). *Methods of soil analysis*. Madison: Soil Science Society of America, 2002. p. 821-826.

REYNOLDS, W. D.; ZEBCHUK, W. D. Use of contact material in tension infiltrometer measurements. *Soil Technology*, Amsterdam, v. 9, n. 1, p. 141-159, 1996.

REYNOLDS, W. D. et al. Comparison of tension infiltrometer, pressure infiltrometer, and soil core estimates of saturated hydraulic conductivity. *Soil Science Society of America Journal*, Madison, v. 64, n. 1, p. 478-484, 2000.

SCHWÄRZEL, K.; PUNZEL, J. Hood infiltrometer: a new type of tension infiltrometer. *Soil Science Society of America Journal*, Madison, v. 71, n. 5, p. 1438-1447, 2007.

SOIL SCIENCE SOCIETY OF AMERICA (SSSA). *Internet glossary of soil science terms*. 2005. Available at: <http://www.soils.org/sssagloss/search.html>. Access on: 18 Nov. 2005.

TIEMEYER, B.; KAHLE, P.; LENNARTZ, B. Nutrient export rates from artificially drained catchments in North-Eastern Germany at different scales. *Agricultural Water Management*, Amsterdam, v. 85, n. 1-2, p. 47-57, 2005.

VANDERLINDEN, K.; GABRIELS, D.; GIRÁLDEZ, J. V. Evaluation of infiltration measurements under olive trees in Córdoba. *Soil Tillage Research*, Washington, DC, v. 48, n. 1, p. 303-315, 1998.

VANDERVAERE, J. P.; VAUCLIN, M.; ELRICK, D. E. Transient flow from tension infiltrometers: I. The two-parameter equation. *Soil Science Society of America Journal*, Madison, v. 64, n. 1, p. 1263-1272, 2000.

WATSON, K. W.; LUXMOORE, R. J. Estimating macroporosity in a forest watershed by use of a tension infiltrometer. *Soil Science Society of America Journal*, Madison, v. 50, n. 1, p. 578-582, 1986.

WHITE, I.; SULLY, M. J. Macroscopic and microscopic capillary length and time scales from field infiltration. *Water Resource Research*, Washington, DC, v. 23, n. 1, p. 1514-1522, 1987.

WOODING, R. A. Steady infiltration from a shallow circular pond. *Water Resource Research*, Washington, DC, v. 4, n. 1, p. 1259-1273, 1968.